

Difference between the cleaved surface and the polished surface on the Raman spectra of $\text{La}_{2-x}\text{Sr}_x\text{CuO}_4$

S. Sugai, Y. Takayanagi, and N. Hayamizu

*Department of Physics, Faculty of Science, Nagoya University, Chikusa-ku, Nagoya 464-8602,
Japan*

(October 22, 2018)

Abstract

The Raman spectra on the cleaved surface of $\text{La}_{2-x}\text{Sr}_x\text{CuO}_4$ is found to be different from those on the mechanically polished or chemically etched surface. On the cleaved surface, the step-like increase of the scattering intensity below 700 cm^{-1} is washed away and the two-phonon peaks are preserved clearly even at the optimum doping. The difference is demonstrated on the optimally doped crystal at $x = 0.15$ and the stripe phase crystal at $x = 0.115$. The stripe phase is stabilized by defects induced by mechanical polishing.

PACS numbers: 74.72.Dn, 78.30.-j, 74.25.Jb, 75.30.Ds, 75.60.Ch

The surface treatment is very important for Raman scattering in high T_c superconductors, because visible light penetrates into the sample by only several hundreds Å from the surface. Up to now the most experiments in $\text{La}_{2-x}\text{Sr}_x\text{CuO}_4$ (LSCO) have been made on the surfaces prepared mechanical polishing or followed by chemical etching with a bromine-ethanol solution [1–8] except for the experiments of antiferromagnetic insulator La_2CuO_4 by Lyons *et al.* [9,10] who used as-grown or cleaved surfaces. In the case of $\text{Bi}_2\text{Sr}_2\text{CaCu}_2\text{O}_{8+\delta}$ (Bi2212), cleaved surfaces have been usually used, because the cleavage is very easy [11–14]. It is known that the cleaved surface is the ideal surface, but it is difficult to obtain a good cleaved surface in LSCO or $\text{YBa}_2\text{Cu}_3\text{O}_{7-\delta}$ (YBCO). We executed Raman scattering on the cleaved surfaces of LSCO selected from a large number of broken flakes of singles crystals. Then we found that the spectra are very different from those of polished or chemically etched surfaces.

We prepared the single crystals at the best condition as far as we could. The single crystals were synthesized by the traveling-solvent floating-zone (TSFZ) method in the infrared-radiation-heating furnace with four oval millers (Crystal system, FZ-T-4000). The melted portion is supported by the surface tension without using a crucible. A ceramic disk (the thickness is 3–4 mm) of LSCO with excess CuO_2 solvent (the ratio among La_2O_3 , CuO , and SrCO_3 is the same as the initial composition of the flax method [15]) is inserted between a single crystal seed and a LSCO ceramic source rod. The solvent disk is heated by focused light and the melted portion is moved at the speed of 1 mm/h. The typical sizes of the single crystal is 4 mm ϕ \times 50 mm length.

This synthesis method ensures the sample free from the contamination of the crucible and the superconducting transition temperature (T_c) is the same as that of the ceramic. Usually single crystals synthesized by the flax method at which the mixture of LSCO and CuO_2 solvent is cooled down slowly in a crucible includes about 0.5 % or more amount of Al or Pt, which reduces the T_c to about 37 K at highest from 42 K of the ceramic LSCO ($x = 0.15$). Moreover the single crystal synthesized by the TSFZ method has uniform Sr concentration, because the Sr concentration in the liquid is kept constant during the crystal

growth by solving the ceramic source with the same Sr concentration. On the other hand the single crystal synthesized by the flax method has different Sr concentration from the center to the surface of the crystal, because the Sr concentration in the liquid changes along the phase boundary between the liquid and the solid as temperature decreases. The quality of the crystal was estimated by the x-ray diffraction, the temperature dependence of the resistivity along the a (or b) axis and the c axis, and the polarized microscope image. There is no impurity phase in the x-ray diffraction. The temperature dependent resistivity is consistent with the reported results for both in-plane and out-of-plane directions [16]. The T_c determined from the mid-point of the transition of the resistivity in the CuO_2 plane is 42 K for LSCO ($x = 0.15$) and 33 K for LSCO ($x = 0.115$). The temperature width between the onset and the end of the superconducting transition is 1.5 K for LSCO ($x = 0.15$) and 2.5 K for LSCO ($x = 0.115$). The cross polarized microscope image of the sample surface shows that the whole area of the sample is composed of the (001) plane. Small holes with a diameter of about a few tens μm were included in some part of the crystal. We measured the Raman spectra in the area free from the holes by monitoring the irradiated sample image through TV camera set in the spectrometer.

The crystal axes were determined by the x-ray Raue pattern. The most part of the crystal rod was cut into many cubes with the sizes $3 \times 3 \times 3$ mm the surfaces of which were perpendicular to the crystal axes. The cubes were cleaved into several tens of pieces. A few pieces with the best condition were used for the Raman scattering measurement. For each Sr concentration, a piece of $3 \times 3 \times 1$ mm was cut and polished by diamond abrasive films successively decreasing the particle diameter from 3, 0.5, to 0.1 μm or from 3, 1, to 0.3 μm in the clean bench. We used n-decane as polishing liquid and hexane as rinse liquid. Hexane gives the better result than methanol or ethanol as for the contamination on the surface, because alcohol easily absorbs moisture. The obtained sample was set in the cryostat and the ambient gas was exchanged to helium within 10 minutes and then the sample was cooled down to 5 K very slowly taking more than 12 hours.

Raman spectra were measured in a quasi-back scattering configuration utilizing a triple

monochromator (JASCO, NR-1810), a liquid nitrogen cooled CCD detector (Princeton, 1100PB), and a 5145 Å Ar-ion laser (Spectra Physics, stabilite 2017). The laser beam of 10 mW was focused on the area of $50 \times 500 \mu\text{m}^2$. The increase of temperature by the laser beam irradiation was less than 2 K at 5 K. The same spectra were measured four times to remove the cosmic ray noise by comparing the intensities at each channel. The wide energy spectra covering $12 - 7000 \text{ cm}^{-1}$ was obtained by connecting 17 spectra with narrow energy ranges after correcting the spectroscopic efficiency of the optical system. The same spot on the surface was measured during the temperature variation by correcting the sample position which was monitored by a TV camera inside the spectrometer.

Figure 1 shows polarized Raman spectra of LSCO ($x = 0.15$) at 5 K and 300 K on the cleaved surface and the polished surface. The final polishing particle diameter is $0.3 \mu\text{m}$. The polarization configuration (xy) denotes that the electric field of the incident light is parallel to the x axis and the scattered light with the electric field parallel to the y axis is detected. The $a = [100]$ and $b = [010]$ directions are parallel to the Cu-O-Cu bonds and the x and y directions are parallel to $[110]$ and $[1\bar{1}0]$. The (xy) spectrum includes the B_{1g} symmetry modes, the (ab) spectrum B_{2g} , the (xx) spectrum $A_{1g} + B_{2g}$, and the (aa) spectrum $A_{1g} + B_{1g}$. The A_{1g} spectrum is obtained by $0.5 \times ((xx) + (aa) - (xy) - (ab))$. The overall spectra are the same for both cleavage and polishing as shown in Fig. 1. However, the superconducting gap structure (discussed later) in all symmetry spectra, many two-phonon peaks from 750 cm^{-1} to 1400 cm^{-1} in the A_{1g} spectrum observed on the cleaved surface at 5 K is missing in the spectra on the polished surface. Instead, the step-like structure emerges below 700 cm^{-1} on the polished surface.

Figure 2 shows the low energy spectra. The intensity of two-phonon peaks at $750-1400 \text{ cm}^{-1}$ decreases in the A_{1g} spectrum, when the surface is polished. Instead, the broad phonon peak appears at 580 cm^{-1} and the scattering intensity shows a step-like increase below 700 cm^{-1} independently of the symmetry. The height of the step decreases to about a half, when the surface is polished by the abrasive film with the diamond diameter of $0.1 \mu\text{m}$. Therefore this structure is attributed to the defect-induced extrinsic phonon peaks. This step-like

structure cannot be removed, even if the surface is etched chemically [7,8]. It indicates that the chemical etching leaves contaminations. The width of the single-phonon peak below about 700 cm^{-1} is much broader on the polished surface than on the cleaved surface.

The superconducting gap structure can be used for the estimation of the surface and the sample quality. Figure 3 shows the B_{1g} , B_{2g} , and A_{1g} spectra at 5K and 40 K and the differential spectra between these temperatures. The B_{1g} electronic Raman spectrum represents the electronic excitation around the $(00) - (\pi 0)$ direction where the d -wave superconducting gap is at the maximum [12,17]. The B_{2g} spectrum represents the excitation around the $(00) - (\pi\pi)$ direction where the gap is at the node. The superconducting gap structure is very clearly observed on the cleaved surface. The peak energies are 204 cm^{-1} for B_{1g} and 112 cm^{-1} for B_{2g} , which are consistent with the results on the chemically etched surface [4,5]. The gap structure disappeared completely on the polished surface.

Figure 4 shows the Raman spectra of LSCO ($x = 0.115$) at 5 K and 300 K on the cleaved surface. The diameter of the final polishing particles is $0.1\text{ }\mu\text{m}$. The T_c decreases at $x = 0.115$ by a few degree from the expected T_c on the T_c vs x curve [18]. This is known as the "1/8 problem". In the case of $\text{La}_{2-x}\text{Ba}_x\text{CuO}_4$ and $\text{La}_{2-x-y}\text{Nd}_y\text{Sr}_x\text{CuO}_4$, the T_c is completely suppressed [18–21]. Tranquada *et al.* [22,23] proposed the stripe structure model in which the antiferromagnetic spin stripes are separated by the charge domain walls. The two-magnon Raman peak at 2373 cm^{-1} at 300 K splits into double peaks at 1910 cm^{-1} and 3037 cm^{-1} at 5 K, as the stripe structure develops at low temperatures. The split of the two-magnon peaks is caused by the different magnetic excitation energy in the two-magnon Raman process near the charge domain walls and in the spin strips. The details will be published elsewhere [24]. The incommensurate split of the magnetic spot at $(\pi\pi)$ has been observed by neutron scattering in the whole range of x in LSCO [25–31]. In Raman scattering, however, the split of the two-magnon peak is observed at very narrow Sr concentration region the width of which is only about 0.01 around $x = 0.115$ in consistent with the decrease of T_c obtained by the electric conductivity and magnetic susceptibility measurements [18]. The narrow Sr concentration makes the observation of the split two-magnon peak difficult. The crystal

synthesized by the TSFZ method has the advantage of the uniform Sr concentration over the crystal made by the slow cooling method. At 300K split two-magnon peaks decreases in intensity and the single two-magnon peak is left in the B_{1g} spectrum of the cleaved surface, but split two-magnon humps are still noticeable in the case of the polished surface. It indicates that the stripe structure is almost vanished on the cleaved surface at 300 K, but is left on the polished surface. The scattering intensity is enhanced, as the stripe structure develops upon decreasing temperature. The strong enhancement of the scattering intensity on the polished surface also indicates that the defects stabilize the stripe structure. The polishing induces the extra phonon peak around 580 cm^{-1} instead of the decrease of the intensity of the two-phonon peaks. The superconducting gap peak is observed in the B_{2g} spectra on the cleaved surface, but not observed on the polished surface.

In conclusion the polished surface loses the superconducting gap structure and the two-phonon scattering intensity. On the other hand the extrinsic phonon peaks appear around 580 cm^{-1} and the scattering intensity increases below it. It causes the defect-induced step-like structure at 700 cm^{-1} in the spectra. The gap structure is recovered by the chemical etching, but the phonon spectrum is retained in the similar structure as on the polished surface. It suggests the importance of the measurement on the cleaved surface, although it needs large single crystals. The stripe structure at $x = 0.115$ is stabilized by the defects induced by polishing.

REFERENCES

- [1] S. Sugai *et al.*, Phys. Rev. B **38**, 6436 (1988).
- [2] S. Sugai *et al.*, Phys. Rev. B **42**, 1045 (1990).
- [3] T. Katsufuji *et al.*, Phys. Rev. B **48**, 16131 (1993).
- [4] X. K. Chen *et al.*, Phys. Rev. Lett. **73**, 3290 (1994).
- [5] X. K. Chen *et al.*, Physica C **295**, 80 (1998).
- [6] J. G. Naeini *et al.*, Phys. Rev. B **57**, R11077 (1998).
- [7] J. G. Naeini *et al.*, Phys. Rev. B **59**, 9642 (1999).
- [8] J. G. Naeini *et al.*, cond-mat/9909342v2.
- [9] K. B. Lyons *et al.*, Phys. Rev. B **37**, 2353 (1988).
- [10] K. B. Lyons *et al.*, Phys. Rev. B **39**, 9693 (1989).
- [11] T. Staufer *et al.*, Phys. Rev. Lett. **68**, 1069 (1992).
- [12] T. P. Devereaux *et al.*, Phys. Rev. Lett. **72**, 396 (1994).
- [13] M. Rübhausen *et al.*, Phys. Rev. Lett. **82**, 5349 (1999).
- [14] S. Sugai and T. Hosokawa, Phys. Rev. Lett. **85**, 1112 (2000).
- [15] S. Uchida et al. Phys. Rev. B **43**, 7942 (1991).
- [16] T. Kimura et al. Physica C **192**, 247 (1992).
- [17] T. P. Devereaux and D. Einzel, Phys. Rev. B **51**, 16336 (1995).
- [18] K. Kumagai *et al.*, J. Mag. Mag. Materials, **76&77**, 601 (1988).
- [19] A. R. Moodenbaugh *et al.*, Phys. Rev. B **38**, 4596 (1988).
- [20] J. D. Axe *et al.*, Phys. Rev. Lett. **62**, 2751 (1989).

- [21] M. K. Crawford *et al.*, Phys. Rev. B **44**, 7749 (1991).
- [22] J. M. Tranquada *et al.*, Nature, **375**, 561 (1995).
- [23] J. M. Tranquada *et al.*, Phys. Rev. Lett. **78**, 338 (1997).
- [24] S. Sugai and N. Hayamizu, submitted to Phys. Rev Lett.
- [25] S-W. Cheong *et al.*, Phys. Rev. Lett. **67**, 1791 (1991).
- [26] T. R. Thurston *et al.*, Phys. Rev. B **46**, 9128 (1992).
- [27] T. Suzuki *et al.*, Phys. Rev. B **57**, R3229 (1998).
- [28] K. Yamada *et al.*, Phys. Rev. B **57**, 6165 (1998).
- [29] H. kimura *et al.*, Phys. Rev. B **59**, 6517 (1999).
- [30] S. Wakimoto *et al.*, Phys. Rev. B **60**, R769 (1999).
- [31] S. Wakimoto *et al.*, Phys. Rev. B **61**, 3699 (2000).

Acknowledgments. This work was supported by CREST of the Japan Science and Technology Corporation.

FIGURES

FIG. 1. (gray) Raman spectra of $\text{La}_{1.85}\text{Sr}_{0.15}\text{CuO}_4$ on the cleaved and the polished surfaces at 5 K and 300 K. The intensity is divided by $n(\omega, T) + 1$, so as to be expressed by the Raman susceptibility, where $n(\omega, T)$ is the Bose-Einstein factor.

FIG. 2. Comparison of the low energy spectra at 5 K between on the cleaved surface and the polished surface of $\text{La}_{1.85}\text{Sr}_{0.15}\text{CuO}_4$.

FIG. 3. Superconducting gap structure on the cleaved surface of $\text{La}_{1.85}\text{Sr}_{0.15}\text{CuO}_4$.

FIG. 4. (gray) Raman spectra in the stripe phase of $\text{La}_{1.885}\text{Sr}_{0.115}\text{CuO}_4$.

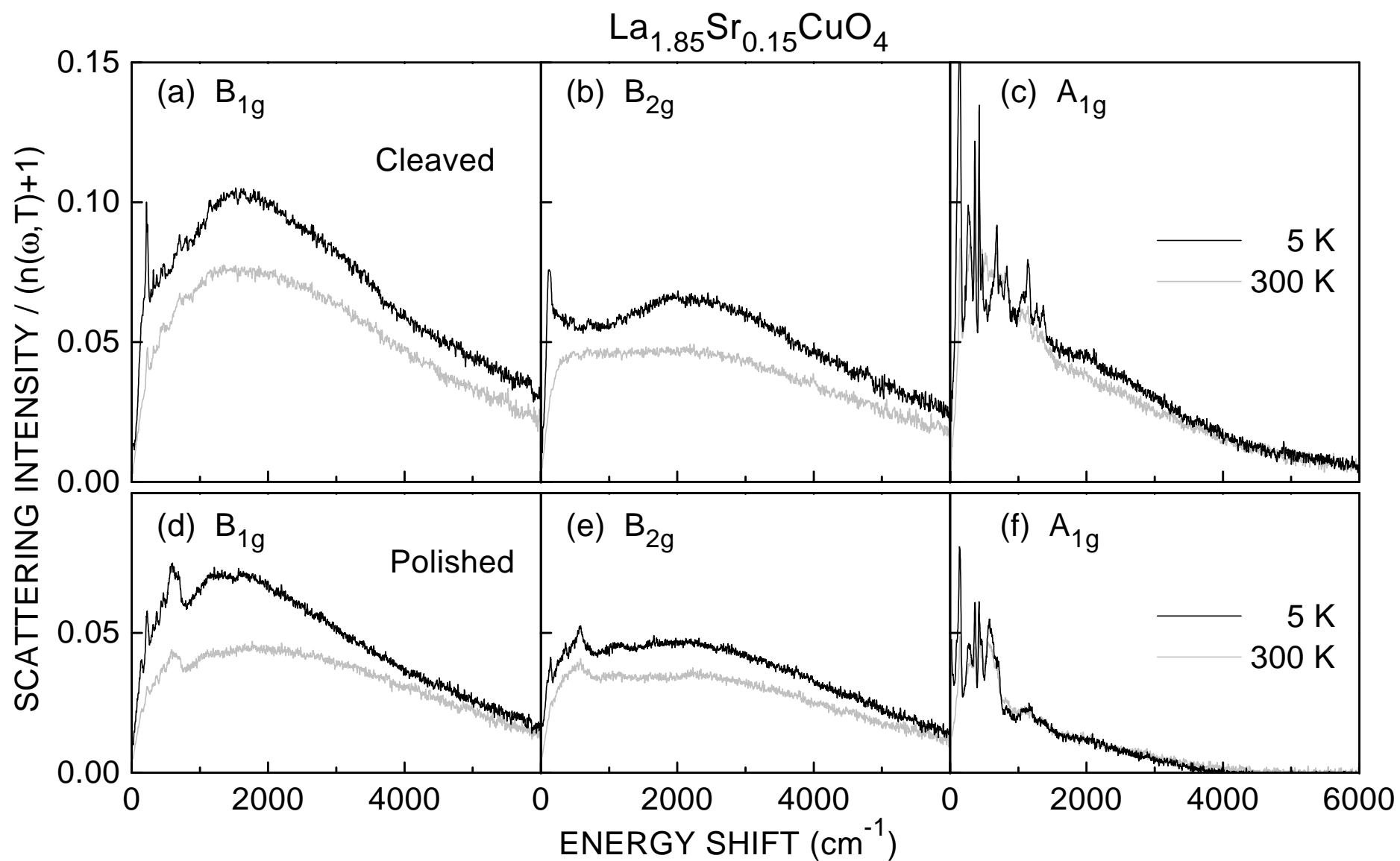


Fig. 1 S. Sugai et al.

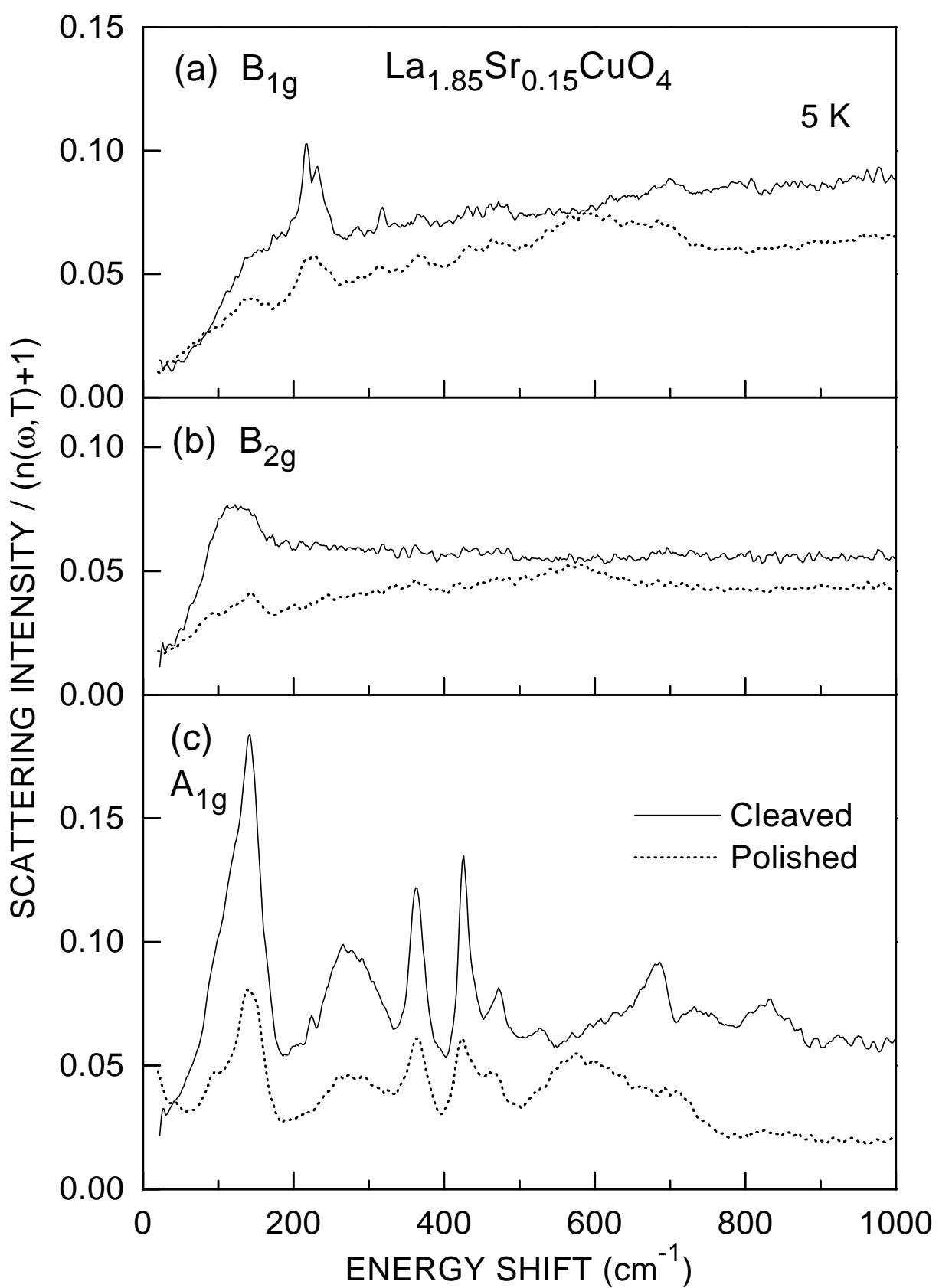


Fig. 2 S. Sugai et al.

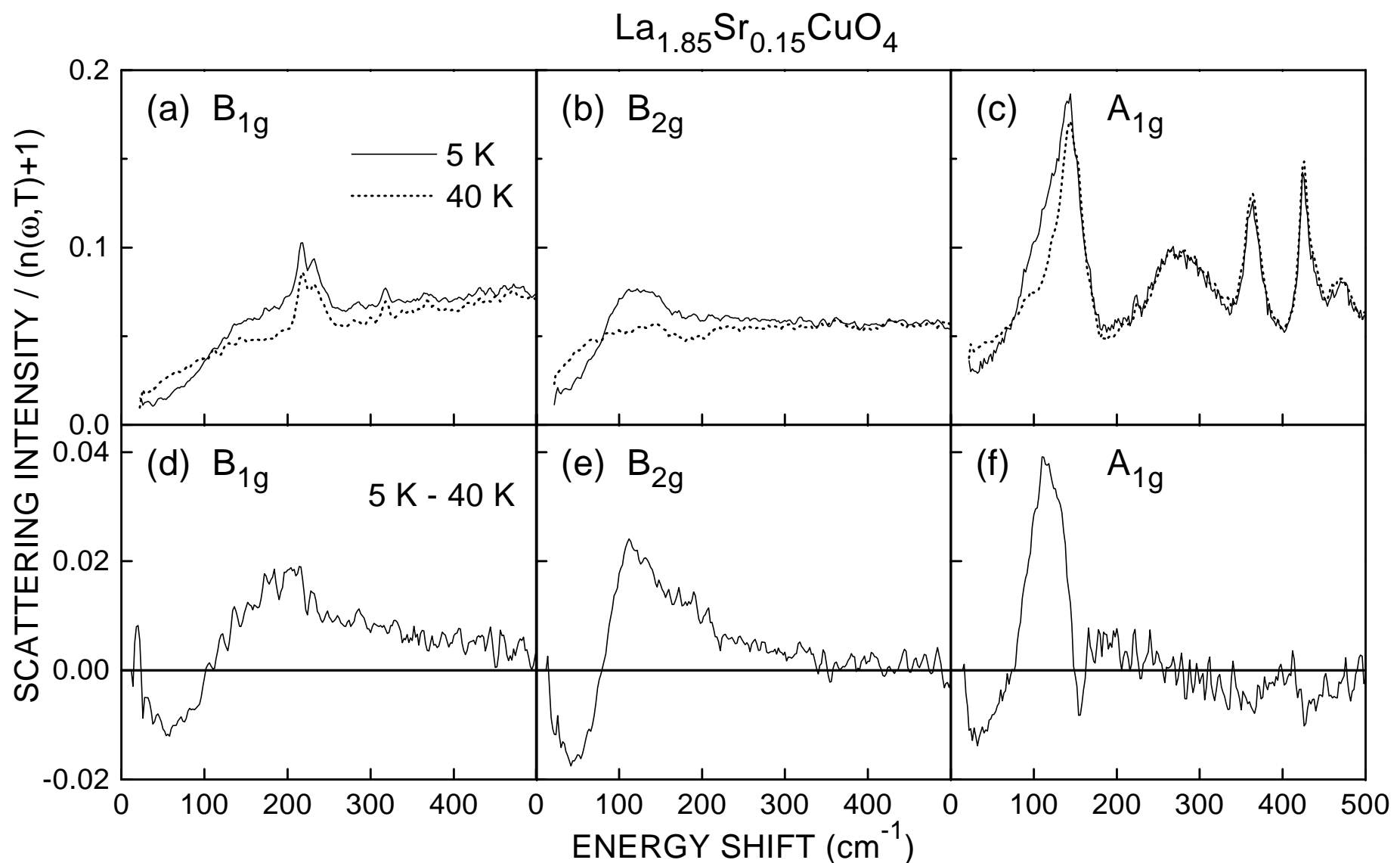


Fig. 3 S. Sugai et al.

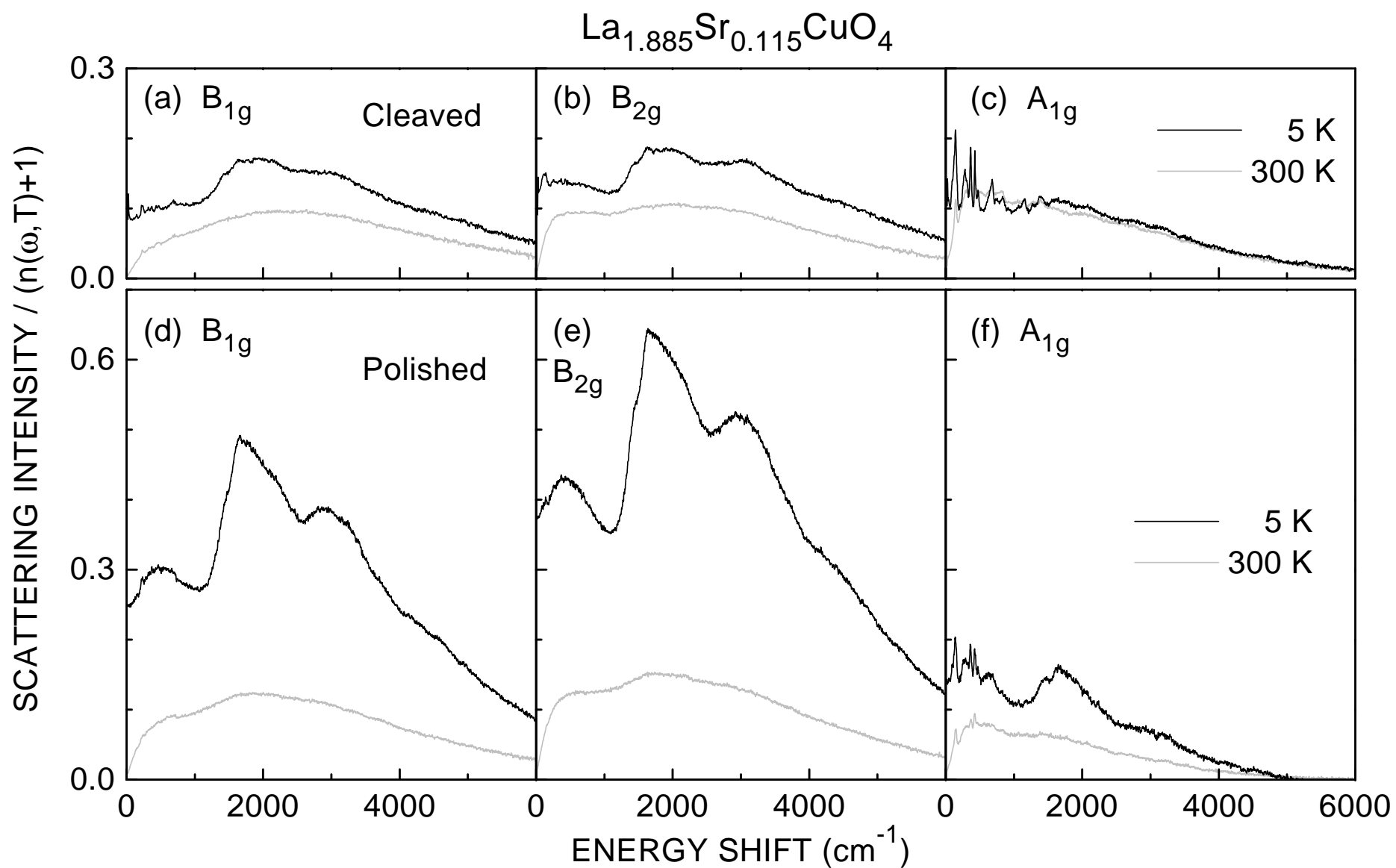


Fig. 4 S. Sugai et al.